Novel Design of Master Manipulator for Robotic Catheter System

Article *in* International Journal of Control Automation and Systems · October 2018

DOI: 10.1007/s12555-018-0089-7

8 authors, including:

Youngjin Moon
University of Florida
26 PUBLICATIONS **45** CITATIONS
SEE PROFILE

Zhenkai Hu
Asan Medical Center
5 PUBLICATIONS **10** CITATIONS
SEE PROFILE

International Journal of Control, Automation and Systems 16(X) (2018) 1-11
http://dx.doi.org/10.1007/s12555-018-0089-7
ISSN:1598-6446 eISSN:2005-4092
http://www.springer.com/12555

Novel Design of Master Manipulator for Robotic Catheter System

Youngjin Moon, Zhenkai Hu, Jongseok Won, Sanghoon Park, Hoyul Lee, Hyeonseok You, Gi-Byoung Nam, and Jaesoon Choi*

Abstract: This paper presents a new master manipulator applied to robotic systems for arrhythmia ablation. The manipulator is designed to implement the concept of two different master-slave teleoperation controls in the clinical application. One is the conventional control between the master and catheter-handle in the slave site and the other is catheter tip manipulation corresponding the master motion. For the purpose, the master has six degrees of freedom (DOF) and consists of three main components: a spherical mechanism for rotational motion of 2-DOF, 3-RRR planar parallel mechanism with 3-DOF, and counter-weight lifting mechanism for the vertical movement. Two mechanisms except the lifting mechanism are parallel chains and structurally more complicated. Therefore, their forward kinematics are analyzed, and workspaces are simulated. To evaluate the applicability for robotic catheter systems, the manipulator prototype was tested for its smoothness, workspace, and teleoperation performance. The subjects in the smoothness test reported no considerable friction and jerk in free movement in the three-dimensional space as shown in the recorded curves. The workspace test shows the actual workspace is similar to the simulated one except some structural constraints in the 3-RRR mechanism. For the last test, a robotic catheter teleoperation system with a slave robot and the software structure for the robotic catheter control system with electrical connection of each component were built. The result performed by five different users shows the motion of the slave robot well tracks that of the master device with small average errors and time delay that are acceptable in robotic catheter teleoperation systems.

Keywords: EP catheter robot, master device, master-slave system, robotic interventional system.

1. INTRODUCTION

Cardiovascular diseases including atherosclerosis, aneurysms, and arrhythmia remain the major cause of mortality worldwide [1–3]. Since the 1990s, endovascular intervention, which uses radiologic imaging device and catheter techniques, has become a common alternative to open surgery for treating cardiovascular diseases [4–8]. In vivo visualization and catheter manipulation are the most basic and essential components of the intervention procedure. X-ray equipment such as fluoroscopy provides the visualization of the heart and the blood vessels to electrophysiologist or cardioradiologist while its radiation negatively affects both patients and clinicians. Although the introduction of three-dimensional (3D) electroanatomic mapping (EAM) systems such as the CARTO (Biosense Webster, Inc., USA) and EnSite (St. Jude Medical, Inc., USA) systems has enabled intraoperative visualization of the catheter in relation to a 3D electrical map and a pre-operatively constructed graphical model of the heart largely reducing the use of fluoroscopy, fluoroscopy is still auxillarilly necessary for the catheter manipulation during procedure.

Robotic catheter systems are to avoid or more reduce

Manuscript received February 12, 2018; revised June 19, 2018; accepted August 2, 2018. Recommended by Associate Editor Chang-Sei Kim under the direction of Editor Myo-Taeg Lim. This work was jointly supported by a grant for the Korea Health Technology R&D Project through the Korea Health Industry Development Institute (KHIDI), funded by the Ministry of Health & Welfare, Korea (grant number: HI14C0517) and by the Basic Science Research Program through the National Research Foundation of Korea (NRF) funded by the Ministry of Education (NRF-2015R1D1A1A01058014). The first two authors contributed equally to this work.

Youngjin Moon is with Department of Convergence Medicine, College of Medicine, University of Ulsan and Biomedical Engineering Research Center, Asan Institute for Life Sciences, Asan Medical Center, Korea (e-mail: jacobian@amc.seoul.kr). Zhenkai Hu and Sanghoon Park are with Biomedical Engineering Research Center, Asan Institute for Life Sciences, Asan Medical Center, Korea (e-mails: hzk7369@gmail.com, sh.park.amc@gmail.com). Jongseok Won is with Graduate School of Convergence Science & Technology, Seoul National University, Korea (e-amil: js1derful@gmail.com). Hoyul Lee was with Biomedical Engineering Research Center, Asan Institute for Life Sciences, Asan Medical Center, Korea and now with Medical Device Development Center, Daegu-Gyeongbuk Medical Innovation Foundation, Korea (e-mail: hoyul.cre@gmail.com). Hyeonseok You is with Department of Biomedical Engineering, College of Medicine, University of Ulsan, Korea (e-mail: neuron1103@gmail.com). Gi-Byung Nam is with Department of Internal Medicine, Heart Institute, Asan Medical Center, University of Ulsan College of Medicine, Asan Medical Center, Korea (e-mail: gbnam@amc.seoul.kr). Jaesoon Choi is with Department of Biomedical Engineering, College of Medicine, University of Ulsan and Asan Medical Center, Korea (e-mail: fides@amc.seoul.kr).
* Corresponding author.

the radiation exposure on patients and physicians while providing augmented dexterity and precision of the cather manipulation, which is expected to result better outcome of the procedure. A robotic catheter system generally consists of a master console as a surgeon-machine interface and a slave robot that follows the commands from the master console to perform the catheterization procedure. Commercial robotic catheter platforms are in two categories depending on the target procedure, vascular and cardiac electrophysiology (EP) intervention. Commercial vascular intervention assist robot platforms include Magellan™ (Hansen Medical, Inc., USA) [9] and CorPath® (Corindus Vascular Robotics, Inc., USA) [10], and the robotic EP catheter systems include Niobe™ magnetic navigation system (Stereotaxis, Inc., USA) [11], Sensei® (Hansen Medical, Inc., USA) [9], Amigo (Catheter Robotics, Inc., USA) [12], and CGCI (Magnetics, Inc., USA) [13]. These systems are at various stages of clinical validation, with systems from Hansen Medical [9], Corindus Vascular Robotics [10] and Stereotaxis [11] currently being clinicaly used at selected sites. Their efficacy in reducing the fluoroscopy time and radiation dosages has been validated by multiple studies [14–16]. While systems from Hansel Medical and Stereotaxis use custom design catheter and accessories causing relatively higher cost and additional training for the handling of the instruments, systems from Corindus Vascular Robotics [10] and Catheter Robotics [12] adopted robot design for the use of conventional catheters and instruments.

In noncommercial domain, some research groups focused on the design of active steearable catheters. In addition to tendon-driven methods [17], steerable catheters driven by shape memory alloys [18], electroactive polymers [19], and hydraulics [20, 21] have also been developed. In addition, Howe's group performed extensive research on catheter motion, as well as the friction and backslash problems during the beating of the heart [22–25]. Patel's group presented studies on the relationship between the bending motion of the tip of an ablation catheter and the motion of the handle knob of the catheter [26, 27]. Most groups have focused on the design of the slave robots but have considered little of the design of the master manipulator. A commercial 3D parallel mechanism universal haptic interface, Falcon (Novint Technologies Inc., USA) has been used often in robotic catheter systems [28–31] due to the merits of low cost and haptic feedback with practical performance. Simple joystick type devices are also used to control catheter robots in both commercial products, e.g., CorPath [10], and by research groups [32]. Thakur *et al.* and Tavallaei *et al.* [8, 17, 33–35] proposed two designs of the master manipulator for conventional nonsteerable catheter/guide wire and standard steerable catheter, respectively. These designs mimicked the catheter manipulation motion of physicians in conventional intervention procedure and focused on the motions of the proximal part or the handle of the catheter. To the best of the authors' knowledge, no research has presented a master manipulator design that focuses on the motions of the catheter tip–the distal part of the catheter that performs the actual treatment action on the surface of subject tissue, inner surface of the atrium or blood vessels.

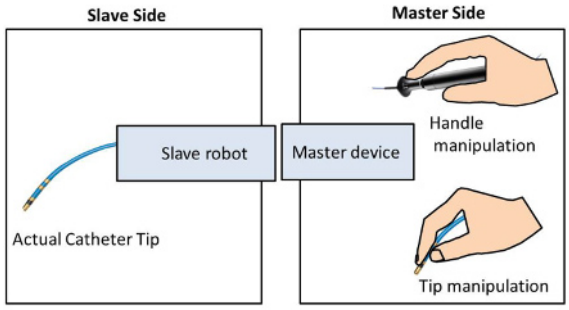

Fig. 1. Concept of the master-slave motion maching.

This paper presents a novel master manipulator for the steerable catheter contol in teleoperative robotic catheter systems. The proposed manipulator can be applied to both types of master-slave motion maching method, maching with the catheter handle and the catheter tip motions (Fig. 1). For the former, six-degrees of freedom (DOF) are sufficient for the master to provide matching motions for the translation, rotation, and bending of the catheter, which are manipulated by the catheter handle in conventional procedure. Current commercial systems and many of research systems adopt this method. In the latter, the physician or electrophysiologist uses the manipulator as if he/she directly controls the motion of catheter tip by virtually gripping it in the hand. Relying on the position and posture information of the distal part of the catheter provided through fluoroscopy or 3D EAM system, physician manipulates the catheter tip to desired position for treatment task such as tissue ablation through the master manipulator. The master manipulator in this case should be designed as a six-DOF mechanism that can fully cover general spatial motion of the control object. Although this method enables more intuitive control of the catheter, the control algorithm of the slave robot becomes more complex problem that requires rigorous modeling of the catheter with its nonlinear dynamic characteristics. For the latter application, the position and posture information of the catheter tip for the slave robot control can be either estimated by mathematical model of the catheter or measured by the 3D EAM system.

The remainder of this paper is organized as follows: The device design including the mechanism design, a direct kinematic analysis, electrical control, and software design are described in Section 2. The evaluation experiments and the results obtained by the device are described in Section 3. Discussions and conclusions are presented

in Sections 4 and 5, respectively.

2. DEVICE DESIGN

2.1. Mechanism design

The mechanical design of the master manipulator is illustrated in Fig. 2. The master manipulator is composed of a planar 3-RRR parallel mechanism, 2-DOF spherical mechanism, and a counterweight lifting device (a 1-DOF linear mechanism). Particularly, the 3-RRR mechanism is attached to a moving block on the closed timing belt of a lifting device, and the spherical mechanism is attached to the moving platform of the 3-RRR mechanism. Seven position sensors (encoders; four for the 3-RRR mechanism, two for the spherical mechanism, and one for the lifting device) are used to calculate the 6-DOF position of the user handle with respect to the base. The resolutions of the encoder are 608, 2000, and 2252 counts per turn in the 3-RRR, spherical, and lifting mechanisms, respectively. In Fig. 2, the moving links are depicted in orange.

The spherical mechanism is a structure that moves on the surface of a virtual sphere whose center is identical to the position of the grip of the mechanism, and the rotation axis of each joint passes through the center. The 3-RRR planar parallel mechanism coupled with the lower end of the spherical mechanism can determine a 2-DOF translational movement in a plane parallel to the ground and a 1-DOF rotational movement perpendicular to the plane. The counterweight lifting device is used to freely move the other two master components in the vertical direction. The counterweight is composed of multiple lead sheets, whose number can be experimentally determined.

2.2. Direct kinematic analysis of the master device

To analyze the direct kinematics of the master device, a global coordinate system with its origin on the base of the master device is defined (Fig. 3). The z-axis of the global coordinate system is collinear with the axis of revolute joint A of the 3-RRR mechanism. The x axis of the global coordinate system is on the base plane and parallel to line AB of the 3-RRR mechanism. The goal of the direct kinematic analysis of the master device is to obtain the position and orientation of the handle with respect to the global coordinate system. In addition to the global coordinate system $\{0\}$, coordinate systems $\{i\}$ with axes of x_i, y_i, and z_i, where $i = 1$, 2, and 3, are defined for kinematic analyses of the linear, 3-RRR, and spherical mechanisms, respectively.

2.2.1 Coordinate transformation from frame $\{0\}$ to frame $\{1\}$

Frame $\{0\}$ is fixed on the base of the master device, and frame $\{1\}$ is obtained by moving frame $\{0\}$ across axis z_0 by a distance d. As d can be measured by the position sensor mounted on the linear mechanism (Fig. 2), the

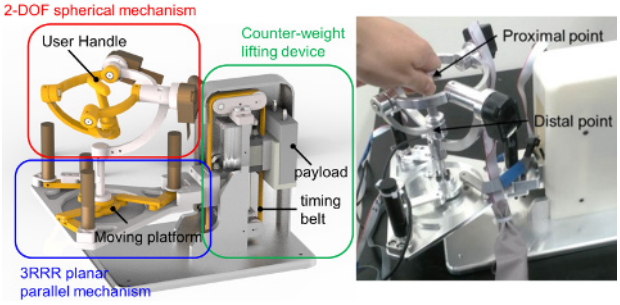

Fig. 2. Mechanical design (left) and prototype (right) of the master manipulator.

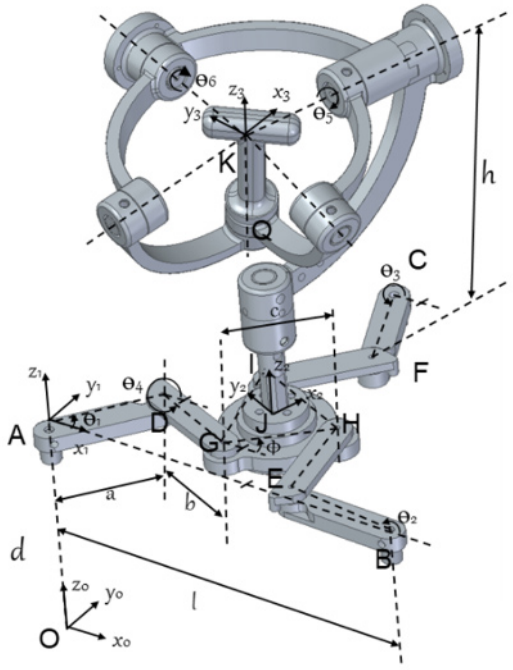

Fig. 3. Coordinate systems for kinematic analyses of the master manipulator.

homogeneous transformation matrix of frame $\{1\}$ with respect to frame $\{0\}$ can be obtained as

$$ {}^{0}_{1}T = \begin{bmatrix} 1 & 0 & 0 & 0 \\ 0 & 1 & 0 & 0 \\ 0 & 0 & 1 & d \\ 0 & 0 & 0 & 1 \end{bmatrix}. \quad (1) $$

2.2.2 Coordinate transformation from frame $\{1\}$ to frame $\{2\}$

The origin of frame $\{2\}$ is fixed at the center–point J of the moving platform of the 3-RRR mechanism–ΔGHI. Axis x_2 of frame $\{2\}$ is parallel to line GJ. Axis z_2 of frame $\{2\}$ is parallel to axis z_1 of frame $\{1\}$. To localize frame $\{2\}$ with respect to frame $\{1\}$, the location of point $J(x, y)$ and the orientation of line GH–angle ϕ in the XY-plane of

frame {1}–must be determined.

Four revolute sensors are used to measure angles θ_1-θ_4 as inputs for calculating $G(x,y)$ and ϕ. An additional sensor is used to measure θ_4 to obtain an analytical solution because no analytical solution can be obtained if only θ_1, θ_2, and θ_3 are used as inputs [36]. $G(x,y)$ can be obtained by solving the vector equation $\overrightarrow{AG} = \overrightarrow{AD} + \overrightarrow{DG}$ with the inputs of θ_1 and θ_4. This vector equation can be expressed as

$$\begin{bmatrix} G_x \\ G_y \end{bmatrix} = \begin{bmatrix} a\cos\theta_1 \\ a\sin\theta_1 \end{bmatrix} + \begin{bmatrix} b\cos\theta_4 \\ b\sin\theta_4 \end{bmatrix}. \tag{2}$$

ϕ can be obtained by solving the following vector equations:

$$\begin{cases} \overrightarrow{HE} = \left(\overrightarrow{AB} + \overrightarrow{BE}\right) - \left(\overrightarrow{AD} + \overrightarrow{DG} + \overrightarrow{GH}\right), \\ |\mathrm{HE}| = \mathrm{b}, \\ \overrightarrow{IF} = \left(\overrightarrow{AC} + \overrightarrow{CF}\right) - \left(\overrightarrow{AD} + \overrightarrow{DG} + \overrightarrow{GI}\right), \\ |\mathrm{IF}| = \mathrm{b}, \end{cases} \tag{3}$$

where $|\mathrm{HE}|$ and $|\mathrm{IF}|$ express the distances of vectors $\overrightarrow{HE}$ and $\overrightarrow{IF}$, respectively. Vector $\overrightarrow{GJ}$ can be obtained by rotating vector $\overrightarrow{GH}$ by $\pi/6$ rad in a counterclockwise direction as follows:

$$\begin{bmatrix} \mathrm{GJ}_x \\ \mathrm{GJ}_y \end{bmatrix} = \begin{bmatrix} \cos\frac{\pi}{6} & -\sin\frac{\pi}{6} \\ \sin\frac{\pi}{6} & \cos\frac{\pi}{6} \end{bmatrix} \begin{bmatrix} GH_x \\ GH_y \end{bmatrix} |GJ| / |GH|. \tag{4}$$

$J(x,y)$ can be easily determined using $\overrightarrow{AJ} = \overrightarrow{AG} + \overrightarrow{GJ}$. Thus, the homogeneous transformation matrix of coordinate system {2} with respect to coordinate system {1} can be expressed by

$${}^1_2T = \begin{bmatrix} \cos(\phi+\frac{\pi}{6}) & -\sin(\phi+\frac{\pi}{6}) & 0 & J_x \\ \sin(\phi+\frac{\pi}{6}) & \cos(\phi+\frac{\pi}{6}) & 0 & J_y \\ 0 & 0 & 1 & 0 \\ 0 & 0 & 0 & 1 \end{bmatrix}. \tag{5}$$

2.2.3 Coordinate transformation from frame {2} to frame {3}

The origin of frame {3} is fixed at the center point of the spherical mechanism–point K, which is located on the z axis of frame {2} at a fixed distance h. Axis z_3 is along the handle of the master device. The orientation of frame {3} with respect to frame {2} can be considered by rotating frame {2} about the x-axis by the angle θ_5, the y axis of frame {2} by the angle θ_6 successively. Therefore, the rotation matrix of frame {3} with respect to frame {2} can be expressed by

$${}^2_3R = \begin{bmatrix} \cos\theta_6 & 0 & \sin\theta_6 \\ 0 & 1 & 0 \\ -\sin\theta_6 & 0 & \cos\theta_6 \end{bmatrix} \begin{bmatrix} 1 & 0 & 0 \\ 0 & \cos\theta_5 & -\sin\theta_5 \\ 0 & \sin\theta_5 & \cos\theta_5 \end{bmatrix}. \tag{6}$$

Thus, the homogeneous transformation matrix of frame {3} to frame {2} can be expressed as

$${}^2_3T = \begin{bmatrix} & & 0 \\ {}^2_3R & & 0 \\ & & h \\ 0 & 0 & 1 \end{bmatrix}. \tag{7}$$

Therefore, the homogeneous transformation matrix of frame {3} to frame {0} can be calculated by combining (1), (5), and (7) as

$${}^0_3T = {}^0_1T \cdot {}^1_2T \cdot {}^2_3T. \tag{8}$$

The workspace of the master device is described as the combination of three component mechanisms. When the distance between A and B in Fig. 3 is given as 150 mm, the workspace of the 3-RRR mechanism with respect to the x-y plane of frame {1} is shown in Fig. 4(a). The green area in this figure is the workspace of the center point of the moving platform of the 3-RRR mechanism and the yellow one is the desired area, which is defined by a circle of diameter 34 mm. The workspace of the user handle on the spherical mechanism with respect to frame {2} is shown in Fig. 4(b). The proximal point of the handle, K in Fig. 3 is at the center of the spherical mechanism. The green area in the figure is the workspace of the distal point of the handle Q, which is 65 mm from the proximal point.

2.3. Electrical and software design of controller

The controller was composed of servo motor controllers, EPOS2 (Maxon Motor, Inc., Switzerland), connected through a controller area network (CAN) backbone to a PC for system monitoring and control.

Object-oriented programming (OOP) was adopted and the software was constructed in modular hierarchical class structure. The CAN communication related functions including sub-functions and parameters for standard CANOpen protocol and Ethernet communication related functions for external communication among the master and the slave robot systems via user datagram protocol (UDP) were contained in dedicated low-level classes. Motor control and kinematics calculation related functions were contained in one high-level class and the classes were functionally connected and operated in the OOP manner. The monitoring and command update time interval of the control loop was 3 ms.

3. EVALUATION EXPERIMENTS AND RESULTS

To evaluate the designed master manipulator, three types of experiments: smoothness, workspace, master-slave teleoperation tests were performed.

3.1. Smoothness test

The motion smoothness in kinematic mechanisms is related to the inertia due to the weight of the links, friction in

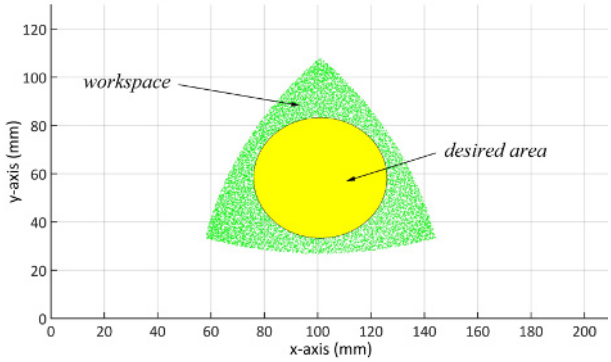

(a)

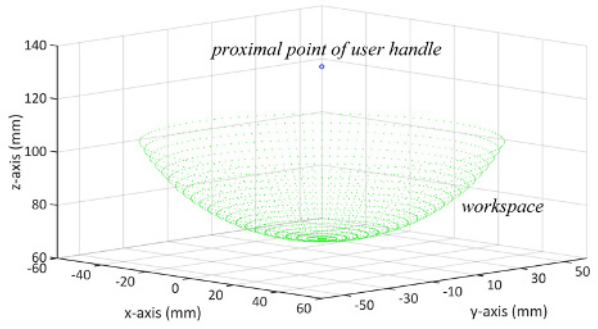

(b)

Fig. 4. Workspaces of the (a) 3-RRR and (b) spherical mechanisms.

joints, backdrivability, position resolution in control, etc. [40, 41]. In human-body motion analysis, various properties for smoothness measurement such as the root mean square jerk are used; however, the best method to quantify smoothness is not available [42]. In this study, the motion continuity of the handle of the device was qualitatively measured to verify its smoothness. The master device was handled by users and moved arbitrarily with an average speed of approximately 35 mm/s. The x, y, and z positions of the distal point of the handle are calculated based on the kinematic analysis described above and recorded automatically in real-time. After recording, the data were plotted using MATLAB (MathWorks, Inc., USA) to observe the trajectory. Five users performed the tests and verbally described the friction felt during the manipulation of the handle. One of the position trajectories of the distal point of the master user handle is plotted in Fig. 5(a). The trajectory appears to be considerably smooth. The distance from a reference point to the user handle of the manipulator is shown in Fig. 5(b). Qualitatively, all users reported that the handle could move freely with negligible friction.

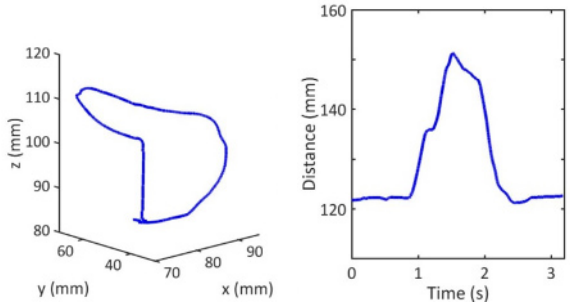

(a) (b)

Fig. 5. (a) Arbitrary position trajectory of the distal point of the master handle and (b) distance change.

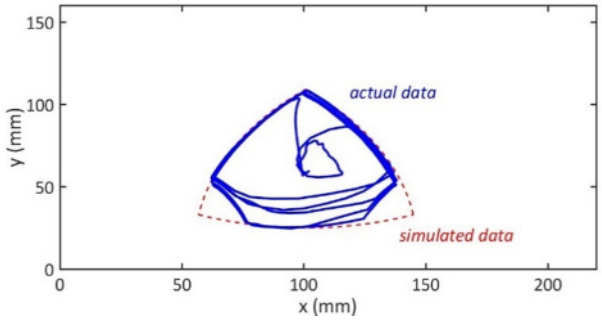

(a)

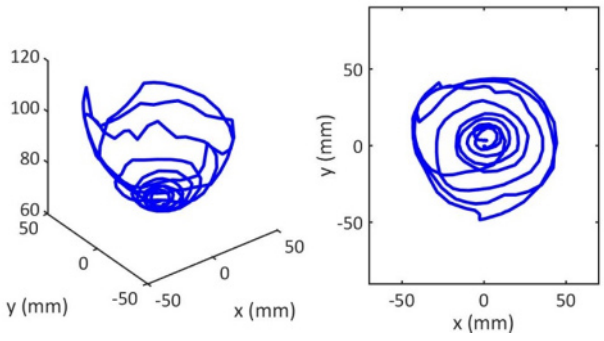

(b)

Fig. 6. Workspace test for the (a) 3-RRR and (b) spherical mechanisms.

3.2. Workspace check

To validate the simulation for the workspace of the 3-RRR planar and spherical mechanisms, the workspace test was performed. For the 3-RRR mechanism, a user is to move the moving platform of the mechanism such that the trajectory would draw the workspace boundary as shown in Fig. 6(a). The difference between the simulated and tested trajectories, both on the bottom side of the triangle, is due to the constraint of the adapters for the encoders in joints D and E of Fig. 3. For the spherical mechanism, a spiral motion was performed and both trajectories in the 3D space and the x-y plane are shown in Fig. 6(b).

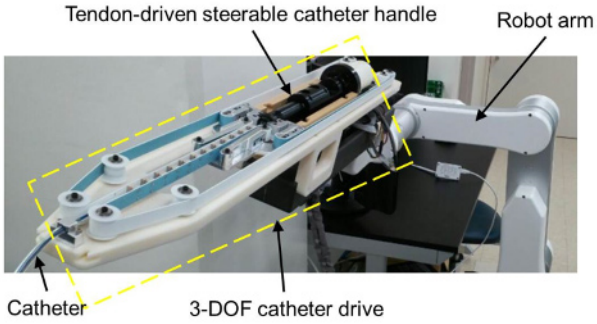

Fig. 7. Mechanical design of the EP catheter robot.

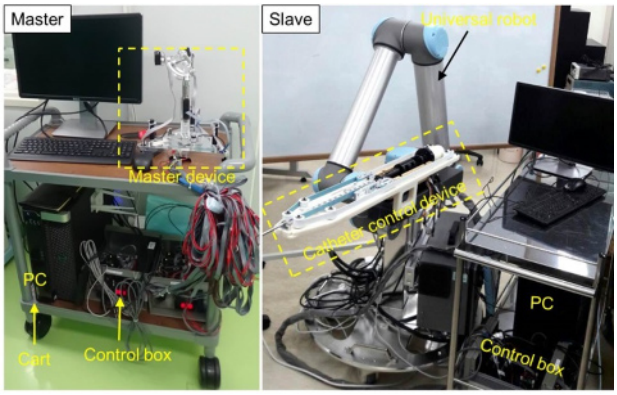

Fig. 8. Masterslave experimental setup.

3.3. Master-slave teleoperation experiment

The master manipulator was tested of the teleoperation using a pre-developed slave EP catheter robot. The details of the slave robot are published in [37]. Briefly, the slave is composed of a tendon-driven steerable EP catheter (Ethicon, USA) and a mechanism to provide 3-DOF motion control for the catheter, including translation, rotation, and tip deflection (Fig. 7). The slave controller can receive commands from any master device via UDP. The master and slave components and controllers were connected via a local area network. The experimental setup is shown in Fig. 8. The master device is used to control the motions of the catheter in free space.

For the teleoperation, the master-slave motion mching is illustrated in Fig. 9. Only three components of the six in the master correspond to the slave catheter drive in this study. The movement of the moving platform of the 3-RRR manipulator along the y_1 and x_1 axes shown in Fig. 3 controls the translation and bending of the catheter, respectively. Rotating the user handle around the z_2 axis controls the rotation of the catheter.

The numerical relation between the master and the slave mentioned above can be defined as follows:

$$v_{tr} = K_{tr} y_K, \tag{9}$$

$$v_{ro} = K_{ro}\,\mathrm{atan2}(y_Q - y_K, x_Q - x_K), \tag{10}$$

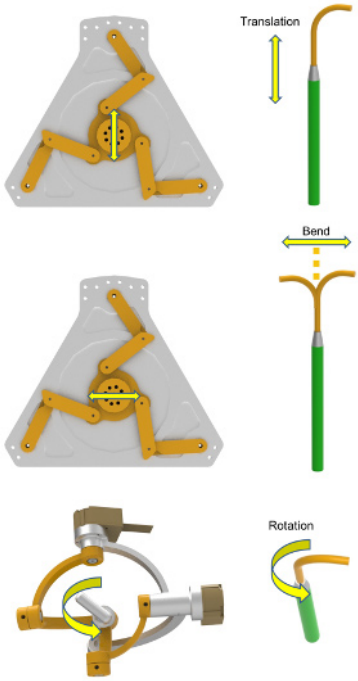

Fig. 9. Master-catheter tip matching concept.

Table 1. Design specification.

	Master	Slave
DOF	6	3
Translation range (mm)	60	60
Rotation range (degree)	180	180
Bend range (mm)	60	18

*Bend range is defined by the displacement of the steerable handle of the catheter used in this study, THERAPY^{TM} COOL PATH (St. Jude Medical, USA), which bends the catheter distal shaft by a push-and-pull action.

$$v_{be} = K_{be} x_K \tag{11}$$

where v_{tr} and v_{ro} are the setting values of the translation distance and the rotation angles of the catheter handle, respectively; v_{be} is the setting value of the moving distance of the steering handle (Fig. 3) of the catheter, which is used to deflect the tip of the catheter; (x_K, y_K) and (x_Q, y_Q) are the positions of the proximal and distal points of the handle, respectively. The scaling coefficients, K_{tr}, K_{ro} and K_{be} are modifiable as inputs in real time during the procedure to adjust the moving speed of the slave. All the three equations in (1) are linear equations, thus one motion in the master can give rise to a unique motion in the slave. The range for translation, rotation and bending motions in both the master and slave is shown in Table 1.

In the experiment, five users were asked to move the user handle of the master manipulator in free space for approximately 1 min. The range of catheter motion that the users attempted to control was set to approximately

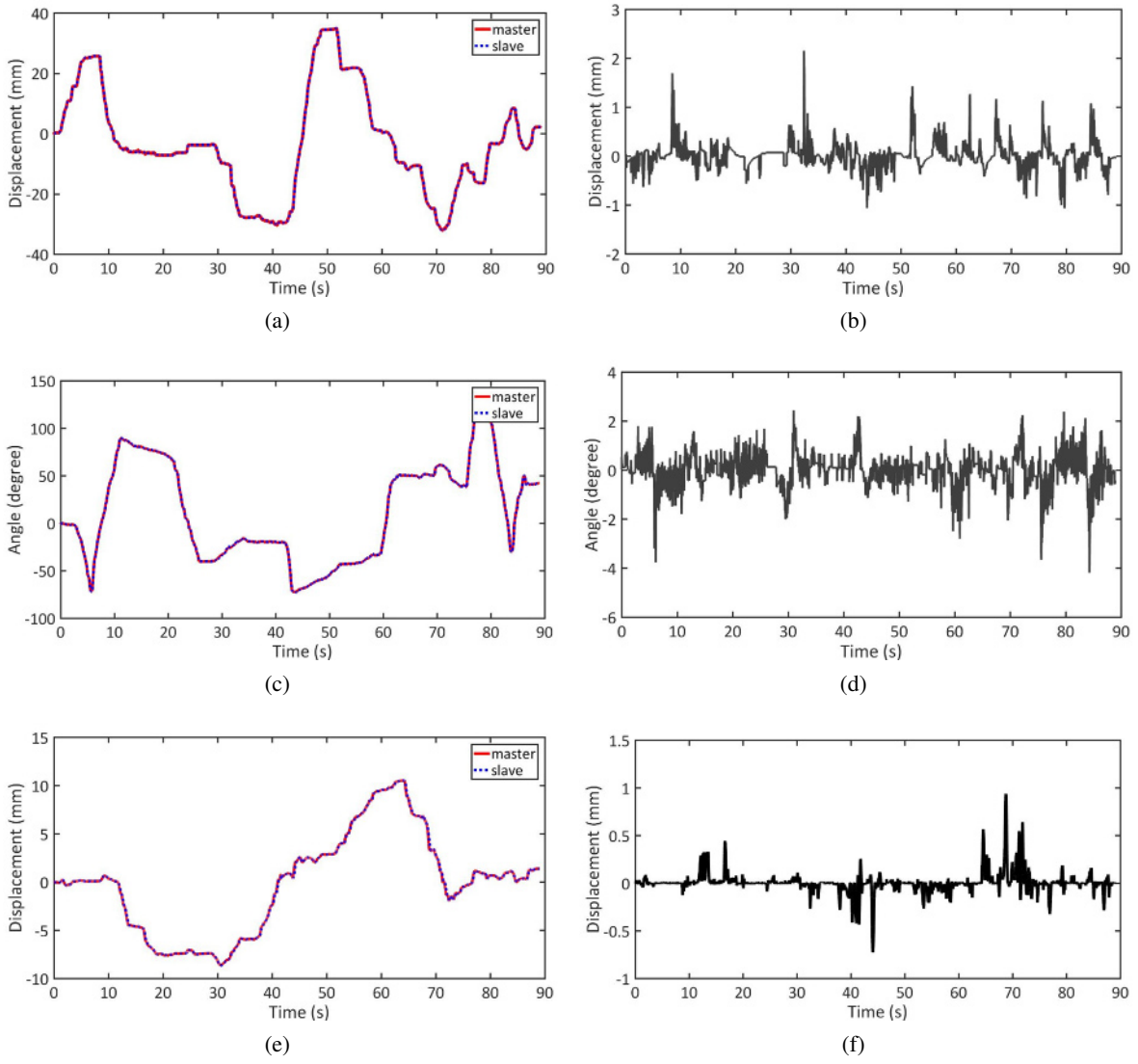

Fig. 10. Real-time data of master-slave experiment: (a) translational motion and (b) error between master and slave, (c) rotational motion and (d) error between master and slave, and (e) translational motion input for bending and (f) error between master and slave.

60 mm in translation and approximately 180° in rotation. They also bent the distal shaft of the EP catheter by controlling the steerable bending knob within a range of 18 mm. The sampling interval of the master motion was 3 ms. The displacements of the slave robot and master were recorded and compared for evaluating the master-slave teleoperation performance.

One data set recorded during the master-slave experiment is shown in Fig. 10. The errors were calculated by subtracting the slave positions from the desired slave positions that were calculated using the master positions. The average errors were 0.25 mm, 0.48°, and 0.073 mm for each full range of motion such as a catheter translation over 65 mm, a rotation over 148°, and the motion of the steerable knob on the catheter handle of over 18 mm, respectively. The results illustrate that the slave moved correctly, following the master.

4. DISCUSSION

In the kinematic design of the master manipulaotor, the forward kinematics of the 3-RRR planar mechanism is used to determine the origin and orientation of the moving platform for a given input that includes the joint angles of three fixed axes. A unique solution could not be obtained from the geometric analytic method. As an alternative for the analytic method, Newton's method can be used as a numerical method to obtain the approximate solutions, but accumulated errors may occur. The analytical solution can be obtained with additional joint angle

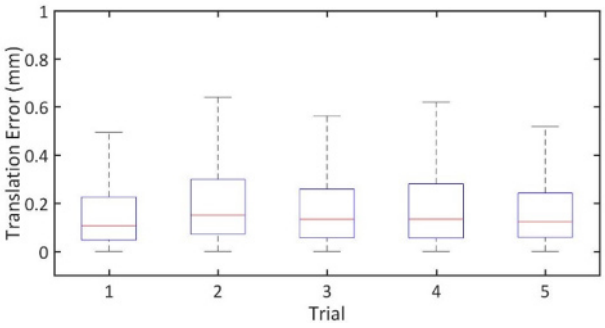

(a)

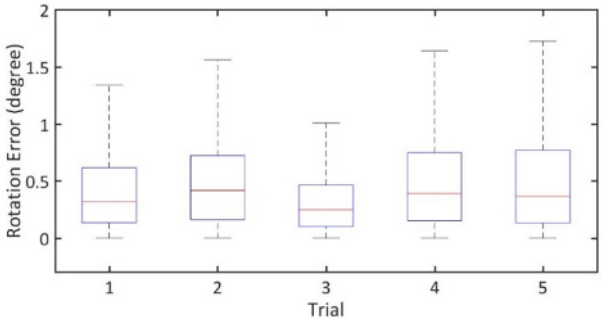

(b)

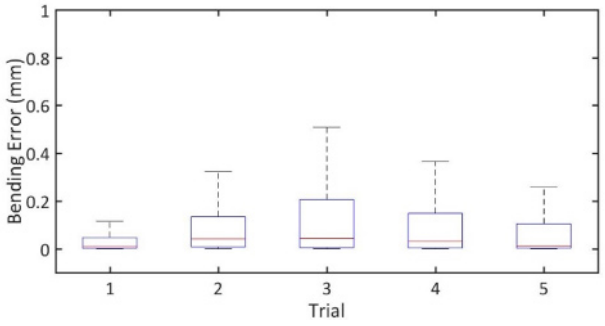

(c)

Fig. 11. Average errors with standard deviations in all the master-slave experiments: (a) translational motion, (b) rotational motion, and (c) translational motion input for bending.

information. Although the possible workspace of the manipulator is calculated as shown in Fig. 4, structural constraints in the actual design of the manipulator prototype yields smaller workspace than the calculated. For the size of the spherical mechanism, a suitable value associated with the radius of the virtual sphere should be determined considering the size of the user hands. The vertical movement caused by the counter-weight lifting mechanism in this study can be replaced with other mechanisms, e.g., a linear actuator.

As shown in Figs. 10 and 11, the reason for the errors appear to be caused by the time delay from the master to the slave for each frame (3 ms) in the robotic system, and the current slave position is in response to the previous master command but not the current command. The use of the master device in this work is limited because the existing catheter robot has only three DOFs. However, if the catheter can arrive at any 3D point and with any posture with improvements in the catheter and slave robot, the tip of the catheter can be considered to have six DOFs, and the master device will be fully used. This is an advantage of the designed master manipulator.

Another advantage is that the master manipulator was designed to control the tip of the catheter to reduce the catheter operating time. However, the existing tendon-driven steerable catheters and catheter robots cannot control a catheter tip arbitrarily; therefore, the user experience of using the master device cannot be fully evaluated yet.

The force feedback in a master device is an issue that needs to be addressed in future work. Most commercial force sensors cannot be mounted on the catheter body because of the small size of the catheters. Guo *et al*. [38] reported a master-slave robotic catheter system mounted with a load cell and torque sensor for the force feedback. In the work of Payne *et al*. [39], small strain gauges were mounted on the catheter body for force feedback. A fiber Bragg grating (FBG) sensor, whose size is smaller than that of a strain gauge, could replace the strain gauges in robotics. Examples of commercial FBG sensors include the products of Micron Optics. However, the cost of FBG sensors limits their application to practical robotic catheters.

5. CONCLUSION

Herein, a novel master device for robotic catheter systems was proposed. The design of the master device enables a user to focus on the manipulation of the tip of the catheter and not the proximal handle of the catheter. The master device has six DOFs and is composed of a 3-RRR planar manipulator, spherical mechanism, and lifting mechanism. A direct kinematic analysis of the master device was analyzed. Both the hardware and software in the system were presented. The device demonstrated a smooth trajectory by observing the dynamic data of the device and obtaining the oral reports from users. Finally, a robotic catheter system was established using the master device and a pre-developed 3-DOF catheter robot.

REFERENCES

[1] R. Lozano, M. Naghavi, K. Foreman, S. Lim, K. Shibuya, V. Aboyans, J. Abraham, T. Adair, R. Aggarwal, S. Y. Ahn, M. A. AlMazroa, M. Alvarado, H. R. Anderson, L. M. Anderson, K. G. Andrews, C. Atkinson, L. M. Baddour, S. Barker-Collo, D. H. Bartels, M. L. Bell, E. J. Benjamin, D. Bennett, K. Bhalla, B. Bikbov, A. B. Abdulhak, G. Bir-

beck, F. Blyth, I. Bolliger, S. Boufous, C. Bucello, M. Burch, P. Burney, J. Carapetis, H. Chen, D. Chou, S. S. Chugh, L. E. Coffeng, S. D. Colan, S. Colquhoun, K. E. Colson, J. Condon, M. D. Connor, L. T. Cooper, M. Corriere, M. Cortinovis, K. C. de Vaccaro, W. Couser, B. C. Cowie, M. H. Criqui, M. Cross, K. C. Dabhadkar, N. Dahodwala, D. De Leo, L. Degenhardt, A. Delossantos, J. Denenberg, D. C. Des Jarlais, S. D. Dhamaratne, E. R. Dorsey, T. Driscoll, H. Duber, B. Ebel, P. J. Erwin, P. Espindola, M. Ezzati, V. Feigin, A. D. Flaxman, M. H. Forouzanfar, F. G. R. Fowkes, R. Frankin, M. Fransen, M. K. Freeman, S. E. Gabriel, E. Gakidou, F. Gaspari, R. F. Gillum, D. Gonzalez-Medina, Y. A. Halasa, D. Haring, J. E. Harrison, R. Havmoeller, R. J. Hay, B. Hoen, P. J. Hotez, D. Hoy, K. H. Jacobsen, S. L. James, R. Jasrasaria, S. Jayaraman, N. Johns, G. Karthikeyan, N. Kassebaum, A. Karen, J-P. Khoo, L. M. Knowlton, O. Kobusingye, A. Koranteng, R. Krishnamurthi, M. Lipnick, S. E. Lipshultz, S. L. Ohno, J. Mabweijano, M. F. MacIntyre, L. Malliger, L. March, G. B. Marks, R. Marks, A. Matsumori, R. Matzopoulos, B. M. Mayosi, J. H. McAnulty, M. M. McDermott, J. McGrath, Z. A. Memish, G. A. Mensah, T. R. Merriman, C. Michaud, M. Miller, T. R. Miller, C. Mock, A. O. Mocumbi, A. A. Mokdad, A. Moran, K. Mullholland, M. N. Nair, L. Naldi, K. M. V. Narayan, K. Nasseri, P. Norman, M. O'Donnell, S. B. Omer, K. Ortblad, R. Osborne, D. Ozgediz, B. Pahari, J. D. Pandian, A. P. Rivero, R. P. Padilla, F. Perez-Ruiz, N. Perico, D. Phillips, K. Pierce, C. A. Pope III, E. Prorrini, F. Pourmalek, M. Raju, D. Ranganathan, J. T. Rehm, D. B. Rein, G. Remuzzi, F. P. Rivara, T. Roberts, F. R. De Leon, L. C. Rosenfeld, L. Rushton, R. L. Sacco, J. A. Salomon, U. Sampson, E. Sanman, D. C. Schwebel, M. Segui-Gomez, D. S. Shepard, D. Singh, J. Singleton, K. Silwa, E. Smith, A. Steer, J. A. Taylor, B. Thomas, I. M. Tleyjeh, J. A. Towbin, T. Truelsen, E. A. Undurranga, N. Venketasubramanian, L. Vijayakumar, T. Vos, G. R. Wagner, M. Wang, W. Wng, K. Watt, M. A. Weinstock, R. Weintraub, J. D. Wilkinson, A. D. Woolf, S. Wulf, P-H. Yeh, P. Yip, A. Zabetian, Z-J. Zheng, A. D. Lopez, and C. JL. Murray, "Global and regional mortality from 235 causes of death for 20 age groups in 1990 and 2010: a systematic analysis for the Global Burden of Disease Study 2010," *The Lancet*, vol. 380, no. 3859, pp. 2095-2128, 2013.

[2] Q. Liu, B. P. Yan, C.-M. Yu, Y.-T. Zhang, and C. C. Poon, "Attenuation of systolic blood pressure and pulse transit time hysteresis during exercise and recovery in cardiovascular patients," *IEEE Transactions on Biomedical Engineering*, vol. 61, no. 2, pp. 346-352, 2014.

[3] Y.-T. Zhang, Y.-L. Zheng, W.-H. Lin, H.-Y. Zhang, and X.-L. Zhou, "Challenges and opportunities in cardiovascular health informatics," *IEEE Transactions on Biomedical Engineering*, vol. 60, no. 3, pp. 633-642, 2013.

[4] D. L. Fischman, M. B. Leon, D. S. Baim, R. A. Schatz, M. P. Savage, I. Penn, K. Detre, L. Veltri, D. Ricci, M. Nobuyoshi, M. Cleman, R. Heuser, D. Almond, P. S. Teirstein, R. D. Fish, A. Colombo, J. Brinker, J. Moses, A. Shaknovich, J. Hirshfeld, S. Bailey, S. Ellis, R. Rake, and S. Goldberg, "A randomized comparison of coronary-stent placement and balloon angioplasty in the treatment of coronary artery disease," *New England Journal of Medicine*, vol. 331, no. 8, pp. 496-501, 1994.

[5] M. Haissaguerre, P. Jais, D. C. Shah, L. Gencel, V. Pradeau, S. Garrigues, S. Chouairi, M. Hocini, P. LE Metayer, R. Roudaut, and J. Clementy, "Right and left atrial radiofrequency catheter therapy of paroxysmal atrial fibrillation," *Journal of Cardiovascular Electrophysiology*, vol. 7, no. 12, pp. 1132-1144, 1996.

[6] M. E. Josephson, *Clinical Cardiac Electrophysiology: Techniques and Interpretations*, Lippincott Williams & Wilkins, 2008.

[7] K. A. Hausegger, P. Schedlbauer, H. A. Deutschmann, and K. Tiesenhausen, "Complications in endoluminal repair of abdominal aortic aneurysms," *European Journal of Radiology*, vol. 39, no. 1, pp. 22-33, 2001.

[8] Y. Thakur, J. S. Bax, D. W. Holdsworth, and M. Drangova, "Design and performance evaluation of a remote catheter navigation system," *IEEE Transactions on Biomedical Engineering*, vol. 56, no. 7, pp. 1901-1908, 2009.

[9] Hansen Medical Inc: http://www.hansenmedical.com/ [Accessed February 2018].

[10] Corindus Vascular Robotics Inc: http://www.corindus.com/ [Accessed February 2018].

[11] Stereotaxis Inc: http://www.stereotaxis.com/ [Accessed February 2018].

[12] Catheter Robotics Inc: http://catheterrobotics.com/CRUS-main.htm [Accessed February 2018].

[13] Magnetics Inc: http://www.magnetecs.com/overview.php [Accessed February 2018].

[14] P. Kanagaratnam, M. Koa-Wing, D. T. Wallace, A. S. Goldenberg, N. S. Peters, and D. W. Davies, "Experience of robotic catheter ablation in humans using a novel remotely steerable catheter sheath," *Journal of Interventional Cardiac Electrophysiology*, vol. 21, no. 1, pp. 19-26, 2008.

[15] M. Koa-Wing, P. Kanagaratnam, D. Wallace, B. Willis, R.A. Kaba, P. Kojodjojo, M. J. Wright, P. B. Lim, N. S. Peters, and D. W. Davies, "Initial experience of catheter ablation using a novel remotely steerable catheter sheath system," *HEART Rhythm*, vol. 4, no. 5, pp. A60-A61, 2007.

[16] M. Schiemann, R. Killmann, M. Kleen, N. Abolmaali, J. Finney, and T. J. Vogl, "Vascular guide wire navigation with a magnetic guidance system: experimental results in a phantom," *Radiology*, vol. 232, no. 2, pp. 475-481, 2004.

[17] M. A. Tavallaei, Y. Thakur, S. Haider, and M. Drangova, "A magnetic-resonance-imaging-compatible remote catheter navigation system," *IEEE Transactions on Biomedical Engineering*, vol. 60, no. 4, pp. 899-905, 2013.

[18] G. Lim, K. Park, M. Sugihara, K. Minami, and M. Esashi, "Future of active catheters," *Sensors and Actuators A: Physical*, vol. 56, no. 1-2, pp. 113-121, 1996.

[19] B.-K. Fang, M.-S. Ju, and C.-C. K. Lin, "A new approach to develop ionic polymer-metal composites (IPMC) actuator: Fabrication and control for active catheter systems," *Sensors and Actuators A: Physical*, vol. 137, no. 2, pp. 321-329, 2007.

[20] K. Ikuta, H. Ichikawa, K. Suzuki, and D. Yajima, "Multi-degree of freedom hydraulic pressure driven safety active catheter," *Proceedings of IEEE International Conference on Robotics and Automation (ICRA 2006)*, 2006.

[21] K. Ikuta, Y. Matsuda, D. Yajima, and Y. Ota, "Pressure pulse drive: A control method for the precise bending of hydraulic active catheters," *IEEE/ASME Transactions on Mechatronics*, vol. 17, no. 5, pp. 876-883, 2012.

[22] S. B. Kesner and R. D. Howe, "Position control of motion compensation cardiac catheters," *IEEE Transactions on Robotics*, vol. 27, no. 6, pp. 1045-1055, 2011.

[23] S. B. Kesner and R. D. Howe, "Robotic catheter cardiac ablation combining ultrasound guidance and force control," *The International Journal of Robotics Research*, vol. 33, no. 4, pp. 631-644, 2014.

[24] P. M. Loschak, L. J. Brattain, and R. D. Howe, "Algorithms for Automatically Pointing Ultrasound Imaging Catheters," *IEEE Transactions on Robotics*, vol. 33, no. 1, pp. 81-91, 2017.

[25] P. M. Loschak, A. Degirmenci, Y. Tenzer, C. M. Tschabrunn, E. Anter, and R. D. Howe, "A four degree of freedom robot for positioning ultrasound imaging catheters," *Journal of mechanisms and robotics*, vol. 8, no. 5, pp. 051016, 2016.

[26] M. Khoshnam and R. V. Patel, "Robotics-assisted catheter manipulation for improving cardiac ablation efficiency," *Proc. of 5th IEEE RAS & EMBS International Conference on Biomedical Robotics and Biomechatronics*, pp. 308-313, 2014.

[27] M. Khoshnam, I. Khalaji, and R. V. Patel, "A robotics-assisted catheter manipulation system for cardiac ablation with real-time force estimation," *Proc. of IEEE/RSJ International Conference on Intelligent Robots and Systems (IROS)*, pp. 3202-3207, 2015.

[28] T. Wang, D. Zhang, and L. Da, "Remote-controlled vascular interventional surgery robot," *The International Journal of Medical Robotics and Computer Assisted Surgery*, vol. 6, no. 2, pp. 194-201, 2010.

[29] C. Meng, J. Zhang, D. Liu, B. Liu, and F. Zhou, "A remote-controlled vascular interventional robot: system structure and image guidance," *The International Journal of Medical Robotics and Computer Assisted Surgery*, vol. 9, no. 2, pp. 230-239, 2013.

[30] G. Srimathveeravalli, T. Kesavadas, and X. Li, "Design and fabrication of a robotic mechanism for remote steering and positioning of interventional devices," *The International Journal of Medical Robotics and Computer Assisted Surgery*, vol. 6, no. 2, pp. 160-170, 2010.

[31] Y. Ganji, F. Janabi?Sharifi, and A. N. Cheema, "Remote controlled robot assisted cardiac navigation: feasibility assessment and validation in a porcine model," *The International Journal of Medical Robotics and Computer Assisted Surgery*, vol. 7, no. 4, pp. 489-495, 2011.

[32] E. Marcelli, L. Cercenelli, and G. Plicchi, "A novel telerobotic system to remotely navigate standard electrophysiology catheters," *Computers in Cardiology*, pp. 137-140, 2008.

[33] Y. Thakur, D. W. Holdsworth, and M. Drangova, "Characterization of catheter dynamics during percutaneous transluminal catheter procedures," *IEEE Transactions on Biomedical Engineering*, vol. 56, no. 8, pp. 2140-2143, 2009.

[34] M. A. Tavallaei, M. Lavdas, D. Gelman, and M. Drangova, "Magnetic resonance imaging compatible remote catheter navigation system with 3 degrees of freedom," *International Journal of Computer Assisted Radiology and Surgery*, vol. 11, no. 8, pp. 1537-1545, 2016.

[35] M. A. Tavallaei, D. Gelman, M. K. Lavdas, A. C. Skanes, D. L. Jones, J. S. Bax, and M. Drangova, "Design, development and evaluation of a compact telerobotic catheter navigation system," *The International Journal of Medical Robotics and Computer Assisted Surgery*, vol. 12, no. 3, pp. 442-452, 2016.

[36] L.-W. Tsai, *Robot Analysis: The Mechanics of Serial and Parallel Manipulators*, John Wiley & Sons, 1999.

[37] Z. Hu, J. Won, Y. Moon, S. Park, and J. Choi, "Design of a Robotic Catheterization Platform With Use of Commercial Ablation Catheter," *Proc. of Design of Medical Devices Conference*, pp. V001T08A005-V001T08A005, 2017.

[38] J. Guo, P. Wang, S. Guo, L. Shao, and Y. Wang, "Feedback force evaluation for a novel robotic catheter navigation system," *Proc. of IEEE International Conference on Mechatronics and Automation*, pp. 303-308, 2014.

[39] C. J. Payne, H. Rafii-Tari, and G.-Z. Yang, "A force feedback system for endovascular catheterisation," *Proc. of IEEE/RSJ International Conference on Intelligent Robots and Systems*, pp. 1298-1304, 2012.

[40] J. Arata, H. Kondo, N. Ikedo, and H. Fujimoto, "Hpatic device using a newly developed redundant parallel mechanism," *IEEE Transactions on Robotics*, vol. 27, no. 2, pp. 201-214, 2011.

[41] S. E. Salcudean and J. Yan, "Toward a force-reflecting motion-scaling system for microsurgery," *Proc. of IEEE International Conference on Robotics and Automation*, pp. 2296-2301, 1994.

[42] S. Balasubramanian, A. Melendez-Calderon, A. Roby-Brami and E. Brdet, "On the analysis of movement smoothness," *Journal of Neuroengineering and Rehabilitation*, vol. 12, no. 112, pp. 1-11, 2015.

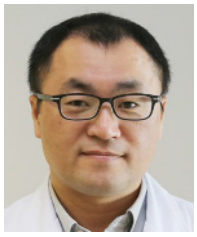

Youngjin Moon received the B.S. and M.S. degrees in control and mechanical engineering and mechanical and precision engineering from Pusan National University, Busan, Korea, in 1996 and 1996, respectively, and the Ph.D. degree in mechanical and aerospace engineering from the University of Florida, Gainesville, FL, USA, in 2011. From 2000 to 2004, he worked for Tanktech Co., Ltd., Busan. From 2005 to 2006, he was a Researcher with the Research Institute of Mechanical Technology, Busan, Korea. He has been a Postdoctoral Researcher with the University of Florida in 2012, and with Asan

Medical Center, Seoul, Korea from 2012 to 2015, respectively. In 2015, he joined Asan Medical Center and University of Ulsan College of Medicine, Seoul, Korea as a Research Assistant Professor. His research interests include design and analysis of kinematic mechanisms, and robotic systems with medical purpose such as surgery, intervention, and rehabilitation.

Zhenkai Hu received the B.S. and M.S. degrees in biomedical engineering from Northeastern University, P.R. China in 2005 and 2007, respectively, and the Ph.D. degree in biomedical engineering from Korea University in 2011. He has been a Postdoctoral Researcher in National Cancer Center, Korea from 2011 to 2015 and in Asan Medical Center, Korea from 2015 to 2018. His research interests include medical robotics and robotic architecture.

Jongseok Won received the B.S. and M.S. degrees in mechanical engineering from Soongsil University, Seoul, Korea, in 1993 and 1995, respectively. From 2007 to 2013, he was a researcher/team manager in Meerecompany Inc., Korea, where he was involved with design and development of laparoscopic surgical robot system. He is currently a Ph.D. candidate in the Department of Transdisciplinary Studies, Graduate School of Convergence Science and Technology, Seoul National University, Seoul, Korea, and a Director of the medical equipment division of NEXTURN Co., Ltd., Korea. His research interest includes design and development of surgical/medical robotic system, interventional robotic system and wearable robots.

Sanghoon Park received the B.S. and M.S. degrees in Biomedical Engineering from Konkuk University, Chungju, Korea, in 2012 and 2014, respectively. He is currently a Researcher at Asan Institue for Life Sciences, Asan Medical Center, Seoul. His research interests include computer-aided surgery and intervention system.

Hoyul Lee received his Ph.D. degree in electronics and system engineering from Hanyang University in 2012. He was a Postdoctoral Researcher with National Cancer Center, from 2015 to 2016, and with Asan Medical Center from 2016 to 2017, respectively. He is currently with the Medical Device Development Center, Daegu-Gyeongbuk Medical Innovation Foundation, Korea as a Senior Researcher. His research interests include design and control of surgical robot, and medical devices.

Hyeonseok You is currently in M.S. course in Department of Biomedical College of Medicine, University of Ulsan, Korea. He received the B.S. degree in Department of Biomedical College of Medicine, University of Ulsan, Korea. His current research interests include machine learning, reinforcement learning, robot control, robotic catheterization, medical training simulation system in virtual reality.

Gi-Byung Nam received the B.M., M.M, and D.M. degrees in medicine from Seoul National University, Seoul, Korea, in 1988, 1997 and 2000, respectively. From 1996 to 1999, he was an Assistant Professor at Choongbuk National University Hospital. He is currently a Professor of the Department of Cardiology, Asan Medical Center and University of Ulsan College of Medicine, Seoul, Korea, and Chair of Atrial Fibrillation Center. His clinical specialty and research interests include cardiac arrhythmias and atrial fibrillation.

Jaesoon Choi received the B.S. degree in control and instrumentation engineering and the M.S. and Ph.D. degrees in biomedical engineering from Seoul National University, Seoul, Korea, in 1995, 1997 and 2003, respectively. He had predoctoral training at the Department of Biomedical Engineering, Lerner Research Institute, Cleveland Clinic Foundation, Cleveland, OH, USA, from 1999 to 2000. From 2004 to 2006, he worked as a Staff Researcher at Research Institute, National Cancer Center, Seoul. From 2007 to 2012, he was a Research Professor at Korea Artificial Organ Center, College of Medicine, Korea University, Seoul. He is currently an Associate Professor of the Department of Biomedical Engineering, Asan Medical Center and University of Ulsan College of Medicine, Seoul. His research interests include computer-aided surgery and intervention, and mechatronics system application in biomedicine.